

# INSPECTION OF REFINERY VESSELS FOR HYDROGEN ATTACK USING ULTRASONIC TECHNIQUES

W. D. Wang  
Shell Development Company  
Westhollow Research Center  
Houston, TX 77082

## INTRODUCTION

Hydrogen attack is a damage mechanism occurring in steels exposed to high pressure hydrogen at elevated temperatures. Under such conditions, hydrogen atoms diffuse into steels and react with carbides. The reaction leads to formation of methane and, subsequently, intergranular fissuring and losses of material strength and toughness.

Detection of hydrogen attack was done previously by measuring echo attenuation [1-4], echo spectrum [2], backscattering amplitude [2-5], velocity [3,4], and velocity ratio [2-4,6]. The first two approaches failed in field inspections because hydrogen attack could not be differentiated from other factors affecting backwall echoes (e.g., grain size, inclusions, cladding, and vessel geometry). The backscattering-amplitude approach eliminates the influences of cladding and vessel geometry but still cannot discriminate hydrogen damage from internal defects such as laminar cracks and inclusions. Measuring velocities is of limited use in the field because it requires measuring material thickness. The velocity ratio approach removes the need of knowing material thickness but effects of cladding on the ratio has never been addressed.

This paper presents improved backscattering, spectrum analysis, and velocity ratio techniques for identifying hydrogen attack. Use of these techniques to quantify the mechanical properties of damaged materials is also presented. Combining techniques in one procedure to expedite field inspections is out of the scope of this paper but can be found elsewhere [7].

## BACKSCATTERING

Scattering of sound waves in hydrogen damaged materials is affected by the intrinsic material properties (e.g., grain size and inclusion content) as well as by hydrogen-attack-induced fissures. Assuming that a material is homogenous before the

attack, one can write the attenuation of sound waves in the material as  $\alpha(x) = \alpha_0 + \alpha_{HA}(x)$ , where  $\alpha_0$  is the intrinsic attenuation coefficient and  $\alpha_{HA}(x)$  is the coefficient of hydrogen-attack-induced attenuation. The  $\alpha_{HA}$  is expressed as a function of distance  $x$  because hydrogen attack inclines to the side of material directly exposed to hydrogen. Thus, the intensity of sound waves in hydrogen damaged material can be written as

$$I(x) = I_0 T e^{-2 \int_0^x [\alpha_0 + \alpha_{HA}(\tau)] d\tau} \quad (1)$$

where  $I_0$  is the intensity of incident sound wave from the transducer,  $T$  is the coefficient of sound energy transmitting through the interface between the transducer and the material, and  $x$  is the distance from the entry surface. Assume that the loss of sound wave energy is mainly due to scattering; similar to the derivation shown by Goebbels [8], it is not difficult to find that the amplitude of backscattering can be approximated as

$$A_S(x) = A_0 T \sqrt{2D[\alpha_0 + \alpha_{HA}(x)] \Delta x} e^{-2 \int_0^x [\alpha_0 + \alpha_{HA}(\tau)] d\tau} \quad (2)$$

where  $A_0$  is the amplitude of the incident sound wave,  $D$  is the fraction of scattering sound energy going in the direction back to the transducer, and  $\Delta x$  is the pulse length.

Equation (2) describes the distribution of backscattering amplitude in the through-wall direction in hydrogen damaged materials. Considering  $\alpha_{HA}$  an index of the severity of hydrogen attack, one can see that hydrogen attack has two opposite effects on the amplitude of backscattering: On one hand, it increases the amplitude through the multiplication term  $\alpha_{HA}(x)\Delta x$ . On the other hand, it decreases the amplitude through the exponential term. The former effect exists because fissures enhances ultrasonic scattering, and the latter due to high ultrasonic attenuation induced by fissuring.

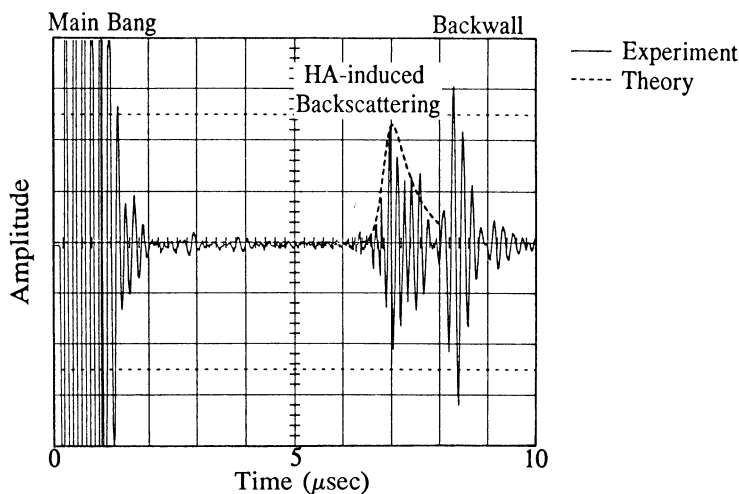
Figure 1 shows an example of results calculated from Eq. (2), in comparison with experimental data. The experimental data were measured from a piece of steel with 20% of wall thickness damaged by hydrogen attack, and the measurement was done from the non-damaged side using a 10 MHz longitudinal wave transducer. The calculation was for the same conditions using Fig 1b as the  $\alpha_{HA}(x)$ . The two results are in good agreement. Both show a rise-and-fall amplitude distribution, as a result of the two effects discussed above — The effect of increasing amplitude dominates at the front end and the effect of attenuation at the rear end of the damage region. Note that the rise of backscattering amplitude coincides the rise of  $\alpha_{HA}$ . The depth at which the amplitude rises, therefore, can be regarded as the damage front for determination of the distance of damage progression.

From an inspection view point, it is important to know that backscattering amplitude can actually be lower in regions of severer damage because of the attenuation effect. Using the absolute amplitude of backscattering to assess the severity of hydrogen damage, therefore, can be quite misleading, especially since the amplitude is also affected by other parameters, as shown in Eq.(2). In contrast, the pattern of the amplitude distribution is more dependent on hydrogen attack and less on the other parameters. To identify hydrogen attack by backscattering measurements, one should therefore rely on the pattern, rather than the absolute backscattering amplitude.

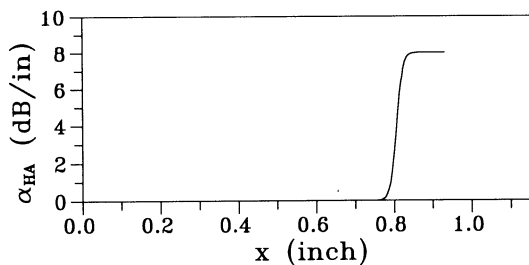
Now let us consider effects of ultrasonic frequency on backscattering patterns. As will be shown later, decreasing frequency decreases  $\alpha_{HA}$ . As shown in Fig. 2, this leads to moving backward the peak position and an increase of the tail amplitude

relative to the peak amplitude. The effect has been proved experimentally, and an example of the results is shown in Fig. 3. As the frequency reduces from 10 to 5 MHz, the tail amplitude increases correspondingly. This frequency dependence provides a useful means in field inspections for differentiating hydrogen damage from midwall inclusions and laminar cracks. In latter cases, decreasing frequency would not increase the tail amplitude.

When the damaged side (e.g., the inside of a vessel) is accessible, backscattering measurements can also be done from the damaged side. Figure 4 shows the theoretical variations of backscattering patterns due to the change measuring direction. Instead of the rise-and-fall patterns, the peaks are pushed to the front and there is only a continuous decrease of backscattering amplitude. Such a change of pattern is confirmed experimentally. An example of experimental results is shown in Fig. 5, where the measurements were done from the inside and outside of a damaged heat exchanger. The drastic change of backscattering pattern due to the change of measuring direction gives us an additional means to discriminate hydrogen attack from inclusions and laminar cracking. In the latter cases, backscattering indications would stay at the same distance to one side of the material regardless of the measuring direction.

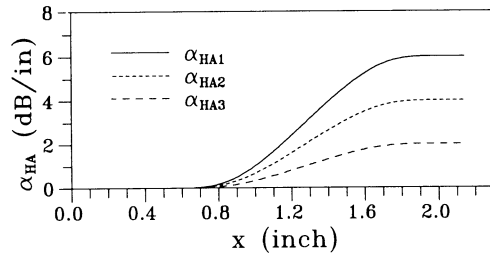


(a)

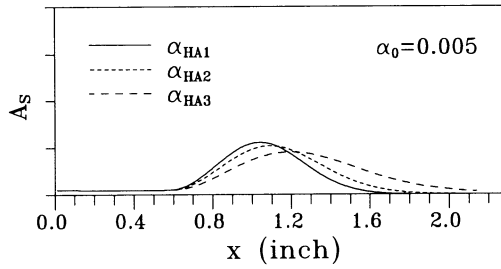


(b)

Fig. 1 (a) Theoretical and measured backscattering amplitude distribution. The measurement was done on a hydrogen-damaged sample from the non-damaged side with a 10 MHz longitudinal wave transducer. The theoretical curve in (a) was calculated from Eq. (2) using  $\alpha_0=0.005$  and the  $\alpha_{HA}(x)$  shown in (b).



(a)



(b)

Fig. 2 Dependence of backscattering patterns on the magnitude of  $\alpha_{HA}$ . The patterns in (b) are calculated from Eq. (2) using  $\alpha_0=0.005$  and the  $\alpha_{HA}$  values shown in (a).

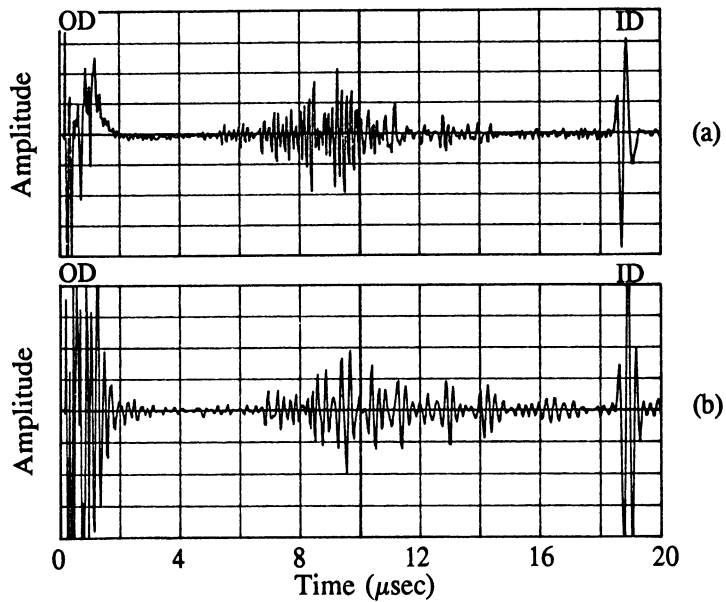


Fig. 3 Results of backscattering measurements on a hydrogen-damaged sample at two ultrasonic frequencies: (a) 10 MHz and (b) 5 MHz.

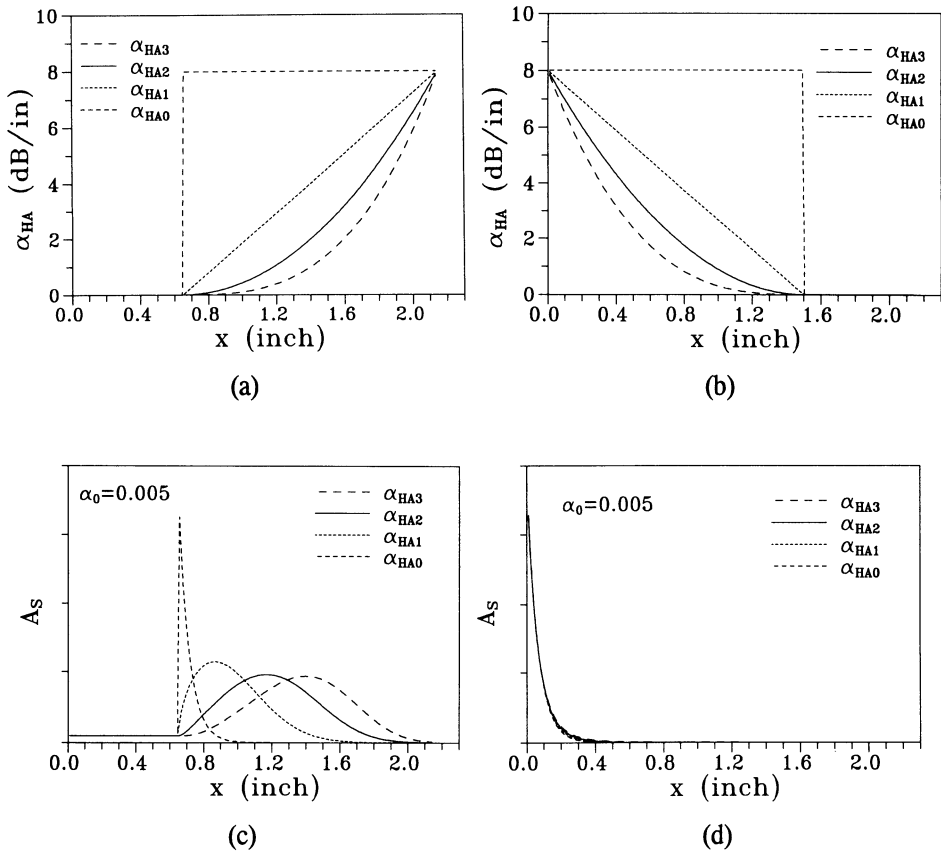


Fig. 4 Theoretical dependence of backscattering amplitude distributions on measuring direction. (c) and (d) are backscattering amplitudes calculated from Eq. (2) using the  $\alpha_{HA}$  distributions shown in (a) and (b), respectively.

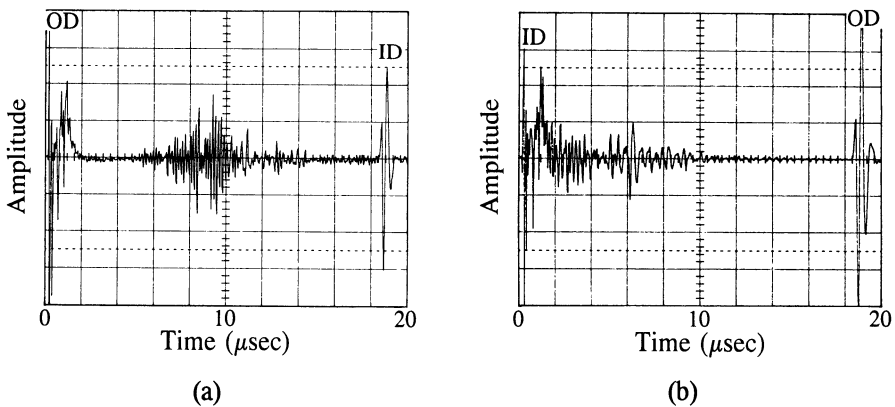


Fig. 5 Backscattering patterns measured from (a) the outside surface (i.e., the non-damaged side) and (b) the inside surface (i.e., the damaged side) of a hydrogen-damaged heat exchanger. The measurements were done with a 10 MHz longitudinal wave transducer.

## SPECTRUM ANALYSIS

Wave scattering at fissures can also be quantitatively assessed through attenuation measurements. Previous attempts [1-4] failed in the field because the effect of hydrogen attack was not discriminated from effects of other parameters such as grain size, inclusions, cladding, and surface geometry. This problem, however, can be solved if we measure attenuation in the frequency domain and use deconvolution to cancel out the effects of other parameters. This can be done by subtracting the spectrum of the first backwall echo in the inspected location from the spectrum of a reference location which has the same metallurgical and structural conditions but without hydrogen damage. The subtraction (i.e., deconvolution) yields a net quantity:

$$20\log\left(\frac{A_{REF}}{A}\right) = (20\log e) \langle \alpha_{HA} \rangle (2d_{HA}) \quad (3)$$

where  $A_{REF}$  and  $A$  are, respectively, the spectra of the reference and inspection locations,  $\langle \alpha_{HA} \rangle$  is the mean value of the coefficient of hydrogen-attack-induced attenuation within the damaged thickness  $d_{HA}$ .

Figure 6 shows an example of spectra measured from clean (i.e., non-damaged) and damaged carbon-0.5Mo steel samples. The deconvolved result (Fig. 6b) reveals a clear increase of attenuation with the increase of frequency. This frequency dependence is useful in identifying hydrogen damage: attenuation that does not increase with the increase of ultrasonic frequency will not be misinterpreted as hydrogen attack. Also, using the distance of damage progression  $d_{HA}$  determined from backscattering measurements, one can calculate  $\langle \alpha_{HA} \rangle$  from Eq. (3) as a measure of the mechanical properties of the damaged material.

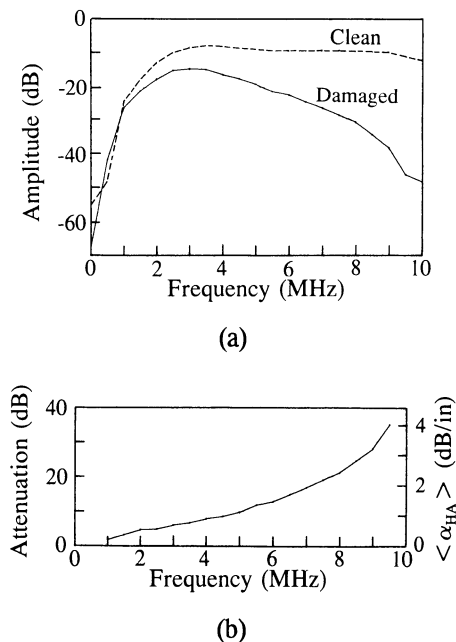


Fig. 6 (a) Spectra measured from clean and through-wall-damaged 0.5" thick C-0.5Mo steel samples. (b) The resultant spectrum from deconvolution. The attenuation in (b) is equal to the  $20\log(A_{REF}/A)$  shown on the left-hand side of Eq. (3).

## VELOCITY RATIO

Velocity ratio measures the ratio of longitudinal-to-shear transit times as the shear-to-longitudinal velocity ratio, i.e.,  $\Delta t_L/\Delta t_S = V_S/V_L$ . The ratio is a function of the Poisson's ratio and, thus, is affected by the material chemistry. In the most severely damaged material that we have experienced, the change of velocity ratio is about 5% (about 7% in previous reports [3,4]), while more than 1% difference can be observed between different materials without damage. When applying the technique on clad equipment, one should therefore measure the time of flight in the base metal instead of the whole wall thickness, so that the effect of cladding is avoided.

## DETERMINATION OF MECHANICAL PROPERTIES

Both  $\langle \alpha_{HA} \rangle$  and  $V_S/V_L$  can be used to quantify the mechanical properties of damaged materials. An example of the correlation between the ultrasonic parameters and mechanical properties is shown in Fig. 7, where the percentage of tensile elongation is plotted against velocity ratio.

Although both  $\langle \alpha_{HA} \rangle$  and  $V_S/V_L$  can be used to assess mechanical properties, they do not have the same sensitivity. Figure 8 shows the relation between  $V_S/V_L$  and  $\langle \alpha_{HA} \rangle$  at 8 MHz. While the attenuation coefficient  $\langle \alpha_{HA} \rangle$  has increased 3 dB/inch, the velocity ratio stays nearly the same, below 0.55. The relation suggests that to assess mechanical properties of damaged materials with high sensitivity one should use attenuation instead of the velocity ratio.

## SUMMARY

This paper discussed three ultrasonic techniques: backscattering, spectrum analysis, and velocity ratio. The backscattering technique identifies hydrogen attack by the rise-and-fall backscattering amplitude distribution. The rise of amplitude coincides the damage front and can be used to determine the distance of damage progression.

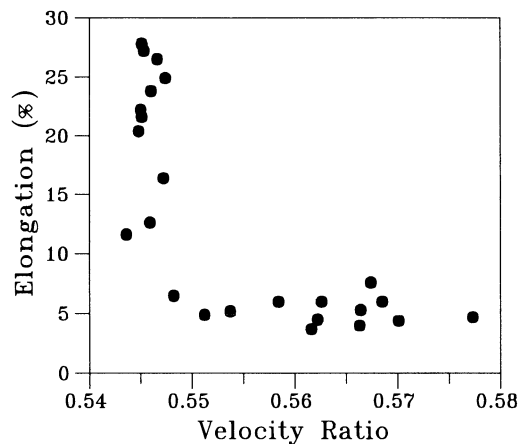


Fig. 7 Percentage of elongation (from tensile tests) versus velocity ratio. The data were measured from hydrogen-damaged C-0.5Mo steel samples.

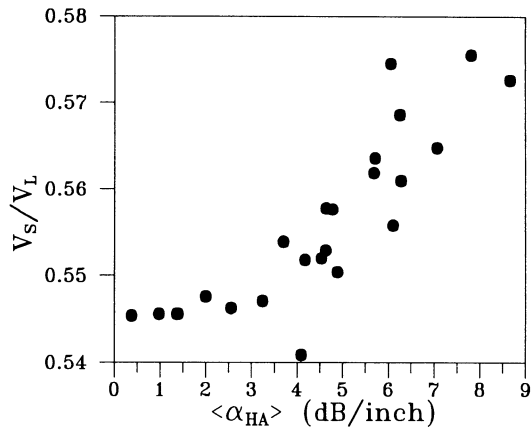


Fig. 8 Relation between  $V_S/V_L$  and  $\langle \alpha_{HA} \rangle$  at 8 MHz. The data were measured from damaged C-0.5Mo steel samples.

The pattern of backscattering amplitude distribution varies with the changes of ultrasonic frequency and measuring direction, which allows us to discriminate hydrogen attack from midwall inclusions and laminar cracks. The spectrum analysis and velocity ratio assist identifying hydrogen attack and can quantify the mechanical properties of damaged materials. The techniques are applicable to vessels with and without cladding.

#### ACKNOWLEDGEMENTS

The author thanks R. A. Cochran, J. T. Reynolds, P. N. Blauvelt, R. C. Hulsey, and M. S. Bell for supporting this research project and tests in the refineries and manufacturing complexes of Shell Oil Company. The author also thank D. V. Rypien for discussions on the spectrum-analysis technique and R. W. Johnson for assistance in measurements.

#### REFERENCES

1. N. O. Cross and A. R. Ciuffreda, Proceedings of American Petroleum Institute, 48th Midyear Refinery Meeting, Los Angeles, CA, May 10, 1983.
2. Y. Hasegawa, Welding International, No. 6, 1988, pp. 41-48.
3. A. S. Birring et al., Materials Evaluation, **47**(3), 1989, pp.345-369.
4. K. Kawano and A. S. Birring, Material Performance, August 1989, pp. 71-74.
5. M. Yajima, D. Shozen, and T. Ohe, Proceedings of American Petroleum Institute, 49th Midyear Meeting, Refining Department V63, 1984, pp. 44-54.
6. T. Watanabe, Y. Hasegawa and K. Kato, in ASTM STP 908, edited by C. C Moran and P. Labine, (ASTM, Philadelphia, PA, 1986), pp. 153-164.
7. W. D. Wang, Technical Progress Report WRC 57-92 (Shell Development Company, Houston, TX, 1992).
8. K. Goebbels, in *Research Techniques in Nondestructive Testing*, edited by R. S. Sharpe, (Academic Press, New York, NY, 1980), Vol. IV, Chap. 4.